

A novel forward problem solver based on meshfree method for electrical impedance tomography

Abstract. In this paper the meshfree method is developed to solve the forward problem for electrical impedance tomography. Differing from finite element method and finite volume method, there is no mesh generation in meshfree method, which is easier to realize and more propitious to be developed as an adaptive procedures for image reconstruction. Numerical simulation results are presented and compared with the results of analytical solution. It is observed that the obtained results are consistent with the results of analytical solution.

Streszczenie. W artykule zaproponowano nową metodę tomograficznej analizy impedancji w której nie generuje się oczek jak na przykład w metodzie elementów skończonych. Dzięki temu uzyskuje się łatwiejszą analizę, w tym także metodami adaptacyjnymi. (Nowa bezczkowa metoda tomografii impedancji elektrycznej)

Keywords: Electrical Impedance Tomography, Forward Problem, Meshfree Method

Słowa kluczowe: tomografia impedancyjna, metoda bezczkowa

1 Introduction

The Electrical Impedance Tomography (EIT) is the process of estimating internal conductivity (changes) through low frequency currents injected into an object and voltages measured at the surface. It was widely applied in fields of biomedicine, geophysics and industry. Compared with the conventional techniques such as X-ray computed tomography (CT) and magnetic resonance imaging (MRI), EIT is conveniently portable and cost effective.

There are two aspects of the EIT problem, forward problem and inverse problem. The forward problem of EIT calculates boundary voltages with the given electrical conductivity distribution, while the inverse problem takes voltage measurements at the boundary to estimate the conductivity distribution. The estimating process is also called as image reconstruction. Almost all approach proposed for EIT reconstruction requires some method to solve the forward problem based on pre-assumed conductivity so that the predicted voltages can be compared with the measured data.

The methods proposed to solve the forward problem include analytical methods, finite difference methods (FDM), boundary element methods (BEM), finite element methods (FEM) and finite volume methods (FVM). While analytical methods are restricted to very simple domains and FDM typically require grids that are topologically regular in some sense, BEM, FEM and FVM are fairly easy to handle arbitrary geometries and boundary shapes.

Although with the BEM only the surface needs to be discretized, but BEM alone can only be used on homogeneous regions, and is useful for fitting impedance values to known regions [1]. To non-homogeneous conductivity distributions on irregular domains problem, the FEM and FVM is more suitable. The comparison between FEM and FVM for EIT forward problem was described in [2]. These methods require an efficient mesh of an object with smooth but irregular surfaces, which respects interior boundaries and electrodes on the surface. The mesh density needs to be determined as a function of position so that high field strengths (for example near electrodes and where conductivity has sharp contrasts) can be accurately represented without excessive density in areas where the field varies slowly [3]. The use of adaptive meshing in both forward and inverse problems was explored in [4], but in practice, it is very time consuming for just trying to develop specific procedures to define the mesh or to properly refine it. Mesh generation is a far more time-consuming and

expensive process than the assembly and solution of the FE or FV equations.

Recently, meshfree methods have become attractive alternatives for problems in computational electromagnetics [5-8]. These methods do not require a mesh to discretize the problem domain. The approximation functions are constructed entirely using a set of scattered nodes, and no element or connectivity of the nodes is needed. Meshfree techniques include two classes: those based on collocations and those based on weak forms. The former is a truly meshfree method and does not require a mesh structure or a numerical integration procedure, but that is less stable and less accurate. Selection of nodes based on the type of a physical problem is still important for obtaining stable and accurate results [9]. The latter include two categories: those require background cells for the integration over the entire problem domain and those require background cells locally for the integration. The methods belonging to the second category are essentially mesh free because creating a local mesh is a simpler task that can be performed automatically without any predefinition for the local mesh [9]. The meshless local Petrov-Galerkin (MLPG) methods belong to this category. Because there is no need to generate a mesh, the nodes can be settled by a computer in a fully automated manner and the nodes can be added or deleted easily whenever and wherever needed, the meshfree method has great potential for solving the difficult problems with complex geometries and the adaptive schemes can be easily developed.

In [10], an approach combined FEM with meshfree method was proposed to solve the forward problem of EIT. The approach used element-free Galerkin (EFG) method based on moving least square (MLS) approximation function to discretize the mesh free region. The EFG method needs background cells for the integration over the entire problem domain. In this paper, a novel MLPG method based on the Radial basis functions (RBF) was developed for the numerical solution of the forward problem for EIT.

The following discussion begins with the local weak form discretization of the forward problem and the calculation with the MLPG method based on the Radial basis functions (RBF-MLPG) in Section 2. The Section 3 gives a numerical example and the result was compared with analytical solution. At the end, conclusions and discussions were given in Section 4.

2 The Solution of Meshfree Method

2.1 The Weak Form of Forward Problem for EIT

In EIT, the potential distribution function u and conductivity distribution function σ in the region Ω are governed by the Laplace equation (1) subject to the boundary condition (2).

$$(1) \quad \nabla \cdot [\sigma(x)\nabla u(x)] = 0 \quad x \in \Omega$$

$$(2) \quad \sigma(x) \frac{\partial u(x)}{\partial \mathbf{n}} = \|j(x)\| \quad x \in \partial\Omega$$

where x is a point in the problem domain, j is the current density applied on the boundary, $\partial\Omega$ is the boundaries of Ω and \mathbf{n} is the unit outward normal vector to the boundary surface. Note that, the injected current in EIT is orthogonal to boundaries. Hence, we define the right part of equation (2) as the module of current density.

The basic idea in MLPG is that the implementation of the integral form of the weighted residual method is confined to a very small local sub-domain of a node. That is

$$(3) \quad \int_{\Omega} \psi_i \nabla \cdot (\sigma \nabla u^h) d\Omega = \int_{\Omega_i} \psi_i \nabla \cdot (\sigma \nabla u^h) d\Omega = 0$$

where u^h is the approximated solution of u and ψ_i (the cubic or quartic spline can be chosen) is the weighted function which define on the sub-domain Ω_i . Integration by parts and application of the Gaussian integration formula lead to

$$(4) \quad \int_{\Omega_i} \psi_i \nabla \cdot (\sigma \nabla u^h) d\Omega = \int_{\Omega_i} \nabla \cdot (\psi_i \sigma \nabla u^h) d\Omega - \int_{\Gamma_i} \nabla \psi_i \cdot (\sigma \nabla u^h) d\Gamma = \int_{\Gamma_i} \psi_i \sigma \nabla u^h \cdot \mathbf{n} d\Gamma - \int_{\Omega_i} \nabla \psi_i \cdot (\sigma \nabla u^h) d\Omega$$

where Γ_i is the boundary of the sub-domain Ω_i and \mathbf{n} is the unit outward normal vector to the boundary Γ_i . If the weighted function was selected in such a way that it vanishes on Γ_i , then in the case of sub-domain Ω_i is located entirely within the global domain Ω , the expression of (4) was changed to

$$(5) \quad \int_{\Omega_i} \nabla \psi_i \cdot (\sigma \nabla u^h) d\Omega = 0$$

and in the case of sub-domain Ω_i intersects with the problem boundary $\partial\Omega$, the expression of (4) would be changed to

$$(6) \quad \int_{\Omega_i} \nabla \psi_i \cdot (\sigma \nabla u^h) d\Omega = \int_{\Gamma_{it}} \psi_i \cdot \|j\| d\Gamma$$

where Γ_{it} is the part of the natural boundary that intersects with the sub-domain Γ_i .

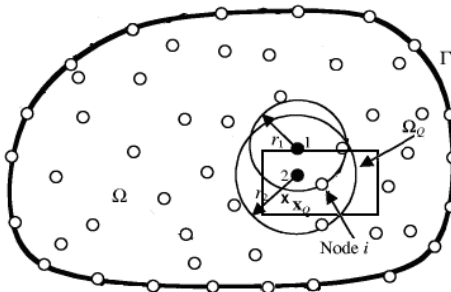


Fig.1. The influence domain and the quadrature domain.

2.2 The Quadrature Scheme

The integrations over the sub-domain in equations (5) and (6) have to be carried out via numerical quadrature techniques. To ensure accurate numerical integration, the Gauss quadrature scheme was used.

In this paper, two types of sub-domain, the influence domain and the quadrature domain, were defined as shown in Fig.1.

The influence domain is defined for each node in the problem domain, as shown in Fig.1, node 2 is included for constructing shape functions for the point marked with x at point x_Q , but node 1 is not included. For the convenience to implement the Gauss quadrature, a rectangle sub-domain Ω_Q was chosen as the quadrature domain of node i . To ensure accurate numerical integration, Ω_Q was divided into 4 cells and for each cell 4×4 Gauss points were selected. By applying the Gauss quadrature scheme, the left hand of the expression of (5) and (6) were changed to

$$(7) \quad \int_{\Omega_i} \nabla \psi_i \cdot (\sigma \nabla u^h) d\Omega = \sum_{n=1}^4 \sum_{p=1}^{16} \nabla \psi_i(x_{Qp}) \cdot [\sigma(x_{Qp}) \nabla u^h(x_{Qp})] A_p = \sum_{n=1}^4 \sum_{p=1}^{16} [\psi_{i,x}(x_{Qp}) u^h_{,x}(x_{Qp}) + \psi_{i,y}(x_{Qp}) u^h_{,y}(x_{Qp})] \sigma(x_{Qp}) \cdot A_p$$

where x_{Qp} is the p th Gauss point in n th cell and A_p is the coefficient of p th Gauss point. The subscript variable i denotes the integration is over the quadrature domain of node i . The subscript variable x or y denotes the partial derivative of the weighted function or the approximated solution.

Compare with the integrations over the sub-domain, the curve integration for boundaries in equations (6) is simpler for EIT forward problem because of j only has value on the injected point and outflow point. So the curve integration value would be

$$(8) \quad \int_{\Gamma_{it}} \psi_i \cdot \|j\| d\Gamma = \begin{cases} 0 & , x_{in} \text{ and } x_{out} \notin \Gamma_{it} \\ -\psi_i(x_{in}) * I & , x_{in} \in \Gamma_{it} \\ \psi_i(x_{out}) * I & , x_{out} \in \Gamma_{it} \\ [\psi_i(x_{out}) - \psi_i(x_{in})] * I & , x_{in} \text{ and } x_{out} \in \Gamma_{it} \end{cases}$$

2.3 The RBF Approximation

In this paper, the RBF approximation procedure was performed to obtain the integrand. The approximate function of u in sub-domain, discretized by a set of nodes which included for constructing shape functions for point x_Q , can be interpolated using radial basis functions as:

$$(9) \quad u^h(x, x_Q) = \sum_{i=1}^n R_i(x) a_i(x_Q) = \mathbf{R}^T(\mathbf{x}) \mathbf{a}(\mathbf{x}_Q)$$

where $R_i(x)$ is the radial basis function in the space coordinates $\mathbf{x}^T = [x, y]$, n is the number of nodes in the neighborhood (refers to the domain of interpolation) of x_Q , and $a_i(x_Q)$ are the coefficients for $R_i(x)$, respectively, corresponding to the given point x_Q .

Enforcing the interpolation to pass through all n scattered points within the sub-domain leads to the following set of equations for the coefficients $a_i(x_Q)$

$$(10) \quad u^h(x_k, x_Q) = \sum_{i=1}^n R_i(x_k) a_i(x_Q) \quad , k = 1, 2, \dots, n$$

which can be expressed in matrix form as follows:

$$(11) \quad \mathbf{U} = \mathbf{R}_Q \mathbf{a}$$

where $\mathbf{U} = [u_1, u_2, \dots, u_n]$ is the vector that collects all the field nodal variables at the n nodes in the support domain and \mathbf{R}_Q is the interpolation matrix of rank $(n \times n)$ as follows:

$$(12) \quad \mathbf{R}_Q = \mathbf{R}_Q^T = \begin{bmatrix} R_1(r_1) & R_2(r_1) & \dots & R_n(r_1) \\ R_1(r_2) & R_2(r_2) & \dots & R_n(r_2) \\ \dots & \dots & \dots & \dots \\ R_1(r_n) & R_2(r_n) & \dots & R_n(r_n) \end{bmatrix}$$

which is a constant matrix for given locations of the n nodes in the sub-domain. Mathematicians have proved that the radial moment matrix R_Q is always invertible for arbitrary scattered nodes [11-13] that is the major advantage of using the radial basis over the polynomial basis.

The coefficients can be obtained as:

$$(13) \quad \mathbf{a} = \mathbf{R}_Q^{-1} \mathbf{U}$$

where \mathbf{R}_Q^{-1} is the inverse matrix of \mathbf{R}_Q . Finally, the interpolation can be expressed as:

$$(14) \quad u^h(x) = \mathbf{R}^T(\mathbf{x})\mathbf{R}_Q^{-1}\mathbf{U} = \Phi(\mathbf{x})\mathbf{U}$$

where $\Phi(\mathbf{x})$ is the shape function defined as:

$$(15) \quad \Phi(\mathbf{x}) = [R_1(x), R_2(x), \dots, R_n(x)]\mathbf{R}_Q^{-1} = [\phi_1(x), \phi_2(x), \dots, \phi_n(x)]$$

2.4 The Calculation with RBF-MLPG

Using Equation (5) or (6) and using Gauss quadrature scheme over the sub-domain, leads to discretized system equations for each node in the problem domain. This gives a set of algebraic equations for each node. By assembling all these sets of equations, a set of discretized system equations for the entire problem domain can then be obtained. Substitution of equation (14) into equation (5) or (6) for all nodes leads to the following discretized system of linear equations:

$$(16) \quad \mathbf{K}\mathbf{U} = \mathbf{f}$$

where \mathbf{K} and \mathbf{f} are "stiffness" matrix and the "load" vector respectively defined as:

$$(17) \quad K_{ij} = \int_{\Omega_i} \nabla \psi_i \cdot (\sigma \nabla \phi_j) d\Omega$$

$$f_i = 0 \quad \text{or} \quad \int_{\Gamma_i} \psi_i \cdot \mathbf{j} d\Gamma$$

Because the influence domain is compact, the system matrix \mathbf{K} produce by MLPG is sparse and the solving procedure of linear equations (16) is efficient.

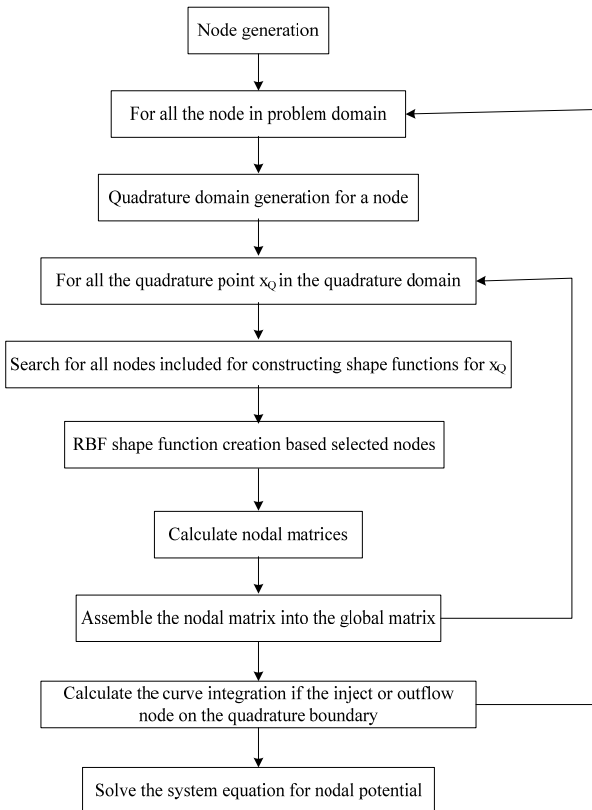


Fig.2. Flowchart of RBF-MLPG method.

The flowchart of the algorithm to solve the forward problem of EIT using the RBF-MLPG method is presented in Fig.2.

3 Simulation Results

In this paper, a model of a 2-D homogeneous ($\sigma=1$) circular was adopted to observe the accuracy of the RBF-MLPG method and to illustrate it's feasibility in solving the EIT forward problem, although the meshfree method has an advantage over FEM lies in it is more effective for the problem with complex geometries and is easier to take an adaptive scheme.

For precise investigation, the following error indicator was used:

$$(18) \quad e = \sqrt{\frac{\sum_{i=1}^N (u_i^{exact} - u_i^{num})^2}{\sum_{i=1}^N (u_i^{exact})^2}}$$

where N is the node number in problem domain, u_i^{exact} is the potential value of node i calculated by the analytical method and u_i^{num} is the potential value of node i calculated by the numerical methods.

For the convenience to compare, the MLPG model was chosen to use the same uniform nodes with the FE model. The relative errors obtained with different dimension were list in table 1.

Table 1. The relative errors obtained with different dimension.

Node Number	Relative Errors	
	MLPG	FEM
37	2.24%	3.87%
81	1.46%	2.37%
177	1.39%	1.47%
217	1.16%	1.30%

It is shown that more accurate estimates of the potential distribution could be obtained with the RBF_MLPG solution.

To test the robust of the proposed method, a scattered 217 nodes model which has the same boundary nodes with the uniform 217 nodes model, as shown in Fig.3, was simulated.

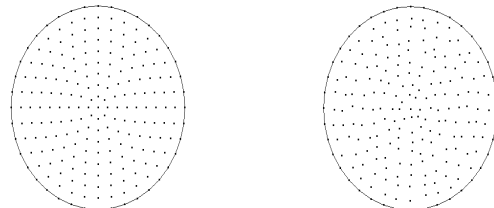


Fig.3. The uniform nodes model (left) and the scattered point model (right).

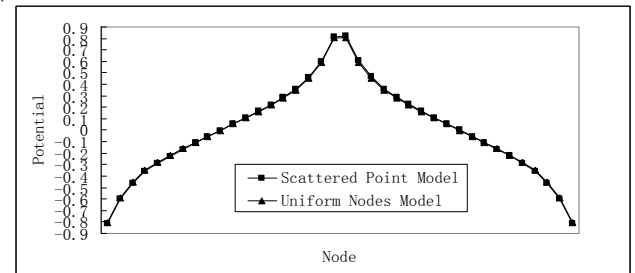


Fig.4. The potential of boundary nodes.

The potential of boundary nodes was shown in Fig.4 and the relative error on the boundary nodes between these two models is 1.98%. It means that stable estimates of the potential distribution can be obtained with the RBF_MLPG solution.

4 Conclusions

The RBF-MLPG method was developed to solve the forward problem for EIT. A local interpolation technique using RBF was used to construct the trial function entirely in terms of a set of scattered nodes. The novelty of the paper is the use MLPG which does not need global domain integration and only integrations on the local domains are needed. Compared to finite element method in transient procedure, MLPG does not need mesh generation which leads to more efficient computations. The results show that MLPG is highly accurate and robust.

The authors gratefully acknowledge the National "111" Project (B08036) and the Project No.CDJXS11151154 supported by the Fundamental Research Funds for the Central Universities.

REFERENCES

- [1] de Munck J C, Faes T J C, Heethaar R M, The boundary element method in the forward and inverse problem of electrical impedance tomography, *IEEE Trans Bio-Med Eng.*, 47(2000), 792-800.
- [2] Dong G Y, Zou J, Bayford R H, Ma X S, Gao S K, Yan W L, Ge M L, The comparison between FVM and FEM for EIT forward problem, *IEEE TRANSACTIONS ON MAGNETICS*, 41(2005), 1468-1471.
- [3] Lionheart W R B, EIT reconstruction algorithms: pitfalls, challenges and recent developments, *Physiol. Meas.*, 25(2004), 125-142.
- [4] Molinari M, High fidelity imaging in electrical impedance tomography, PhD thesis, (2003), University of Southampton.
- [5] Guimares F G, Saldanha R R, Mesquita R C, Lowther D A, Ramirez J A, A meshless method for electromagnetic field computation based on the multiquadric technique, *IEEE TRANSACTIONS ON MAGNETICS*, 43(2007), 1281-1284.
- [6] Viana S A, Mesquita R C, Moving least square reproducing kernel method for electromagnetic field computation, *IEEE TRANSACTIONS ON MAGNETICS*, 35(1999), 1372-1375.
- [7] Viana S A, Rodger D, Lai H C, Meshless local Petrov–Galerkin method with radial basis functions applied to electromagnetics, *IEE Proc.-Sci. Meas. Technol.*, 151(2004), 449-451.
- [8] Zhang Y, Shao K R, Guo Y G, Zhu J G, D. Xie X, Lavers J D, An improved multiquadric collocation method for 3-D electromagnetic problems, *IEEE TRANSACTIONS ON MAGNETICS*, 43(2007), 1509-1512.
- [9] Liu G R, Meshfree Methods: Moving Beyond the Finite Element Method, CRC Press, New York 2003.
- [10] Cutrupi V, Ferraioli F, Formisano A, Martone R, An approach to the electrical resistance tomography based on meshless methods, *IEEE TRANSACTIONS ON MAGNETICS*, 43(2007), 1717-1720.
- [11] Powell M J D, The theory of radial basis function approximation in 1990, *Advances in Numerical Analysis*, Oxford University Press, Oxford 1992.
- [12] Schaback R, Approximation of polynomials by radial basis functions Wavelets, Images and Surface Fitting, A K Peters Ltd., Wellesley, MA 1994.
- [13] Wendland H, Error estimates for interpolation by compactly supported radial basis functions of minimal degree, *J. Approx. Theor.*, 93(1998), 258-272.

Authors: Dr. HU Gang, Prof. CHEN Minyou, Prof. HE Wei and Dr. ZHAI Jinqian, State Key Laboratory of Power Transmission Equipment & System Security and New Technology, School of Electrical Engineering, Chongqing University. No. 174, Shazhengjie, Shapingba District, Chongqing 400044, China. E-mails: gang.hu.cq@gmail.com minyouchen@cqu.edu.cn hewei@cqu.edu.cn and jinqianzhai@163.com.

The correspondence address is: Gang HU, State Key Laboratory of Power Transmission Equipment & System Security and New Technology, School of Electrical Engineering, Chongqing University. No. 174, Shazhengjie, Shapingba District, Chongqing 400044, China.
e-mail: gang.hu.cq@gmail.com.